LEVEL II

12

OPTICAL EXCISION PROGRAM

HOLOGRAPHIC LOCAL OSCILLATOR

PSI-ER-5538-01

(9) Rept. for 28 Dec 78-31 Jul 79

PROBE SYSTEMS, INCORPORATED
655 NORTH PASTORIA AVENUE
SUNNYVALE, CALIFORNIA

(11) Jul 79

(6) OPTICAL EXCISION PROGRAM.
HOLOGRAPHIC LOCAL OSCILLATOR.

(14) PSI-ER-5538-01

(12) 36

ARPA Order Number: 3621
Program Code Number: 8E20
Effective Date of Contract: 28 December 1978
Contract Expiration Date: 31 August 1980
Reporting Period: 28 December 1978-31 July 1979
Contract Number: N00039-79-C-0141
Principal Investigator: (10) Dave Jackson, (408)732-6550

DARPA/NAVELEX JOINT PROGRAM
Sponsored By
Defense Advanced Research Projects Agency
ARPA Order No. 3621
Sponsored and Monitored By
NAVELEX Under Contract (15) N00039-79-C-0141,
JJARPA Order-3621

409007 fm

The views and conclusions contained in this document are those of the authors and should not be interpreted as representing the official policies, either expressed or implied, of the Defense Advanced Research Projects Agency or the U.S. Government.

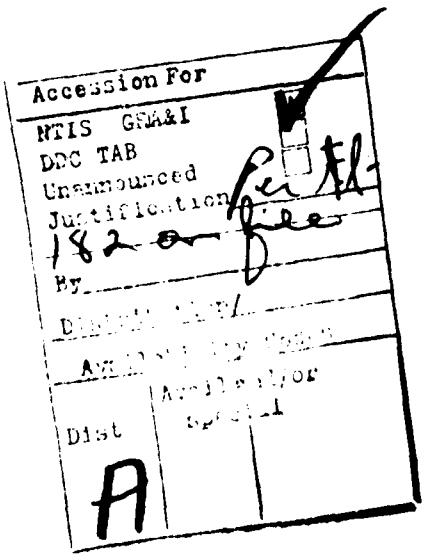

TABLE OF CONTENTS

LIST OF ILLUSTRATIONS

EXECUTIVE SUMMARY

A new technique for coherently detecting optical signals has been demonstrated in the laboratory. Prior to this work, conventional interferometer techniques were the only method by which the amplitude and phase of an optical signal could be measured, but the mirrors and beam-splitters required careful alignment and introduced a susceptibility to microphonic noise and laser coherence effects. Reported here are the results of an effort to design, process, and evaluate holograms capable of producing the optical local oscillator needed in coherent, realtime optical signal processors.

For more than a decade it has been known that an optical spectrum analyzer that has an acousto-optical input transducer can reconstruct the signal by coherently detecting the signal spectrum. This type of processor provides the capability to continuously form the spectrum of a signal, modify the signal spectrum, and then output a time-waveform signal reconstructed from the modified spectrum. This capability has been overlooked for the past decade partly because of the modest performance of the optical components needed in the processor. Recent advances in Bragg cell and detector technology now permit the development of wideband, high-resolution optical processors with performance orders of magnitude beyond that forecasted for future digital signal processors.

Coherent detection optical processors have also been held back by the need to split off some of the light from a very coherent laser and then recombine the local oscillator light with the optically generated signal spectrum. This local oscillator beam needed beam-splitters and mirrors that required careful alignment and very high stability. The movement of one of the components as small as one third micron (about ten microinches) would cause a complete phase reversal of the output signal. Unless the local oscillator and spectrum path lengths were closely matched, a very coherent laser was required. These special needs of a coherent detection optical processors discouraged applications outside the laboratory.

PROBE Systems invented an alternate approach to the generation of an optical local oscillator beam and preliminary experiments with a holographic lens indicated that the approach had considerable promise to eliminate problems associated with the conventional beam-splitter technique. The effort reported here was supported as part of the Joint Navy/DARPA Optical Excision Program and the purpose of this task was to determine the feasibility of an optical local oscillator formed by a hologram lens. Analytical and experimental investigations showed that a holographic local oscillator eliminated the need for vibration sensitive mirrors and beam-splitters. Since the local oscillator and spectrum beams travel down the same path, laser coherence requirements are relaxed and the effects of air currents are greatly reduced. The optical processor dynamic range was measured both with the holographic lens and with the mirrors/beam-splitters local oscillators and the holographic approach proved to be equal to the conventional approach.

Future efforts should concentrate on investigations of non-linear effects and diffraction efficiencies of holographic local oscillators as a first step in the development of engineering design data to be used in future coherent-detection optical processors. When the performance of the holographic local oscillator technique is better qualified, it should be possible to design, fabricate, and display rugged optical processors suitable for modern signal environments encountered by a variety of military platforms.

SECTION 1
INTRODUCTION

1. INTRODUCTION

This special technical report describes the successful demonstration of a holographic technique that holds considerable promise for providing a noise-free local oscillator in coherent detection optical processors. This effort is one part of a DARPA/NAVELEX Joint Program for the development of the techniques and technology needed to implement an interference excisor subsystem for broad-band receivers.

Optical excision is a signal processing technique for eliminating narrowband RF interference signals and has many potential applications in the areas of broadband communications, radar, and intercept systems. This technique uses an acoustical-optical Bragg cell and a continuous laser to form the spectrum of an electrical input signal. The optically generated spectrum of the signal allows the processor to block strong narrowband interference signals and by coherently detecting the remainder of the spectrum, an interference-free electronic broadband signal is obtained as the output of the processor. The successful development of optical excisor technology would permit the exploration of a whole family of optical coherent processors that would, in real time, allow access to the spectrum of a broadband signal.

The unique feature of the excisor processor is the output signal, which is a coherent time-domain electronic signal reconstructed by the coherent detection of the optical signal spectrum. The coherent detection technique does, however, require the generation of an optical local oscillator or reference beam. In a laboratory environment this requirement can be easily met with a few beam-splitters and mirrors; but in a small, rugged, rack-mounted package, the stability of the local oscillator beam can be degraded by vibration and thermal effects. A noisy LO beam would limit the coherence of the electronic output signal and hence limit the usefulness of an optical excisor.

1. --Continued

The purpose of the task reported here was to investigate the feasibility of using holographic techniques to generate the optical local oscillator beam needed for coherent detection of the optical spectrum. The principal advantage of a holographic local oscillator is the elimination of the conventional beam-splitters and mirrors along with their interferometric stability and alignment requirements.

The technical approach for this analytical and experimental effort was to first identify and specify the characteristics desired of a hologram that would generate an interferometer quality optical local oscillator. This was followed by a series of experiments where high resolution photographic plates were exposed to optically generated interference patterns and then processed to form holograms.

The local oscillator holograms were measured individually and as part of a coherent optical signal processor. The diffraction efficiencies of the best holograms ranged between 1.5 and 2.7 percent which was determined to be adequate for achieving optimum performance. When a hologram was used in an optical spectrum analyzer, the maximum output signal-to-noise ratio in a 30 KHz noise bandwidth was 47 dB, which is within 2 dB of the maximum signal-to-noise ratio when the beam-splitter and mirrors were used to generate the local oscillator. Measurements of the phase distortion, frequency response, and spurious signals showed that the holographic technique did not degrade the performance of the optical processor.

The holographic local oscillator proved to be very stable and free of amplitude and phase noise. The hologram replaces two beam-splitters and two mirrors and eliminates the problems associated with the alignment and vibration of those components. Also because the holographic local oscillator beam and the optical signal beams travel nearly identical paths, phase and amplitude differences caused by thermal effects are greatly reduced.

1. --Continued

This successful demonstration of the feasibility of using holographic techniques to generate an optical local oscillator has also identified areas that will need additional work. A new techniques development program could address issues such as the limitations to higher diffraction efficiencies, spurious signals due to photographic film nonlinearities, and could provide the engineering data needed in the design of rugged, practical optical excisors.

SECTION 2
HOLOGRAM PREPARATION

2. HOLOGRAM PREPARATION

This section of the report describes the design and preparation of the holograms used in the experiments discussed in Section 3. The apparatus used to expose the holograms is described along with the analysis of hologram placement. The photographic processing and diffraction efficiency measurements are presented in enough detail to permit duplication by other researchers.

2.1 HOLOGRAM CONSTRUCTION

The apparatus used to expose the holograms is basically the same as the optics used in the interferometer method of coherent detection (Figure 1). The laser light passing through the Bragg cell is combined with the reference and transformed with a lens. If an electronic signal were applied to the Bragg cell, the detector would produce an output whose amplitude is proportional to the input signal.

The purpose of the hologram is to essentially record, in the way of a photograph, the interference pattern between the two laser beams. When reilluminated with one of the original beams, the other beam is reconstructed according to the principles of diffraction.* The shutter in Figure 1 provides a means to control the amount of light energy that falls upon the photographic plate and the variable beam-splitter and optical attenuator provide an adjustment of the ratio of the reference to signal beams during exposure. Thirty holograms were exposed with different exposure levels and ratios of reference to signal beams. The majority of these were also exposed with the Bragg cell removed from the optical path in order to avoid the Fresnel effects caused by the aperture edge.

*In the case of the optical local oscillator, some of the dc beam which would normally come to a focus on the optic axis is actually diffracted onto the detector. This diffracted beam then serves as the reference in the coherent detection technique.

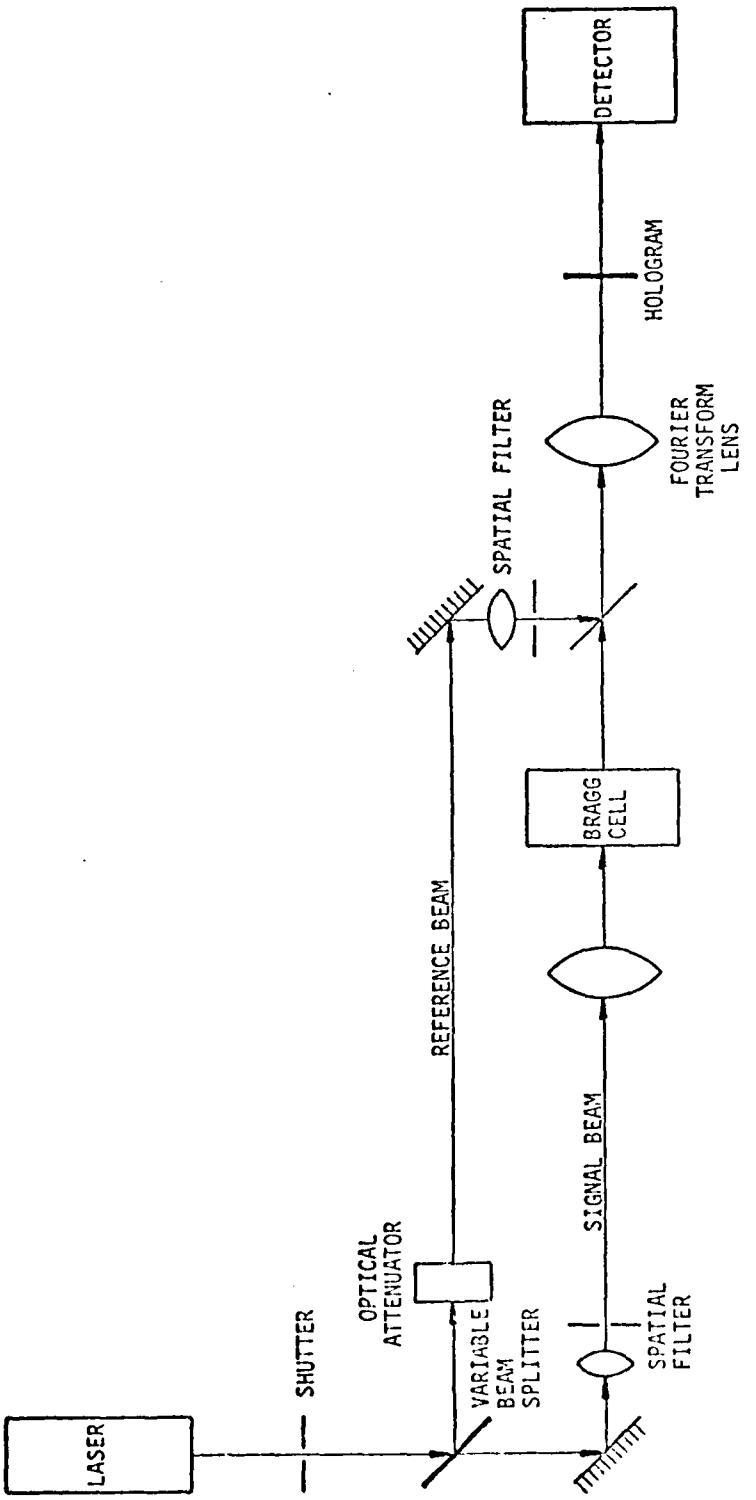

FIGURE 1 HOLOGRAM EXPOSURE SET-UP

2.1 --Continued

Figure 2 illustrates the use of the processed hologram to generate the optical local oscillator beam. With no signal input to the Bragg cell, the only light falling upon the hologram is the undiffracted or dc beam. Upon visual inspection, a reference can be observed at the detector plane. Replacing the hologram back to the exact location where it was originally exposed is easily accomplished by applying a signal to the Bragg cell and finely adjusting the holograms position until the detector's output is better for no other position. The original placement of the hologram was determined using the results of the following analysis.

2.2 HOLOGRAM PLACEMENT

Figure 3 depicts a closer look at detection with the use of a holographic local oscillator. The dotted lines trace the path of a typical optical signal, the solid lines depict the Bragg cell undeflected beam and the dashed lines represent the path that the reference follows as observed by the detector. Other parameters shown are defined as follows:

h MAX $\triangleq$ vertical distance to the top most part of the hologram utilized, the lowest portion through which the dc beam must pass in order to deflect a reference onto the entire detector aperture.

y MAX $\triangleq$ the vertical distance to the top of the dc beam at distance x.

y MIN $\triangleq$ the bottom of the dc beam such that y MAX - y MIN is equal to the net height of the beam at x.

b $\triangleq$ the vertical distance to the point where the upper frequency signal falls upon the detector.

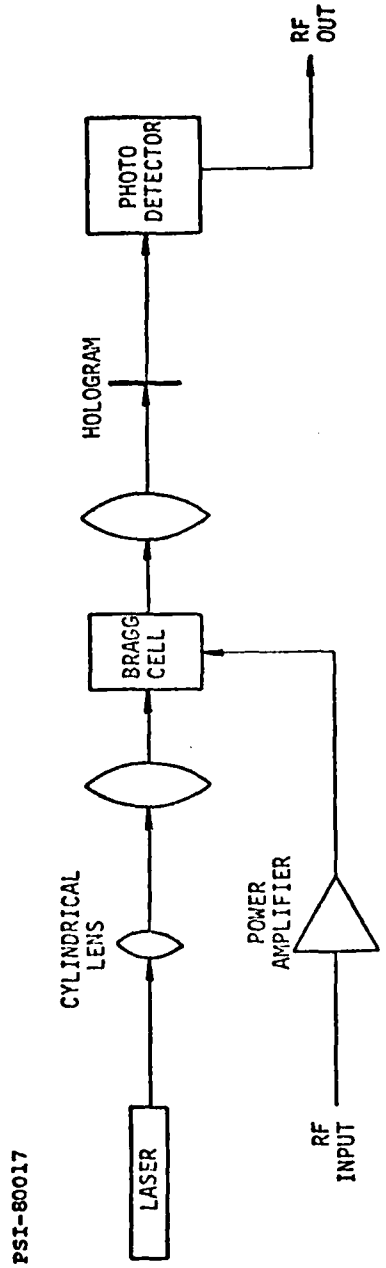

FIGURE 2 COHERENT DETECTION WITH HOLOGRAPHIC LOCAL OSCILLATOR

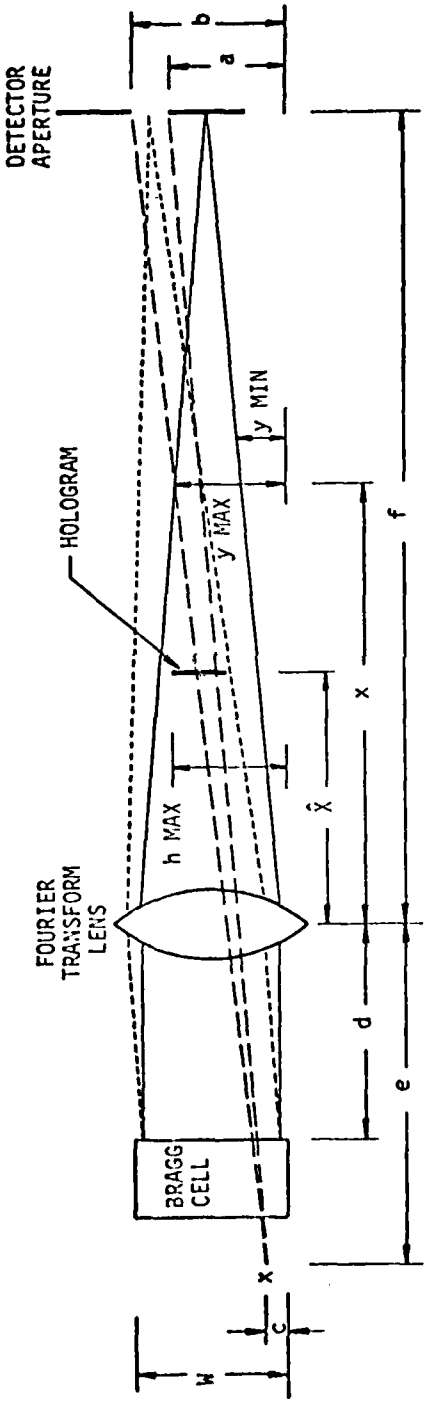

FIGURE 3 HOLOGRAM PLACEMENT

2.2 --Continued

c $\triangleq$ the spatial distance to the virtual focal point of the reference.

d $\triangleq$ the distance between the Bragg cell and the Fourier Transform lens.

e $\triangleq$ virtual focus of the reference.

f $\triangleq$ focal length of the Fourier Transform lens.

w $\triangleq$ width of the Bragg cell aperture.

x $\triangleq$ distance to the hologram.

The shaded portion in the figure at the distance $\hat{x}$ shows where the hologram can be placed so as to provide a reference to the entire detector aperture. The percentage of the dc beam utilized or falling upon the hologram can be shown to be equal to the following:

$$K \triangleq \frac{\frac{b - a}{f + e}(e + \hat{x})}{\frac{W}{F}(f - \hat{x})}$$

$\hat{x}$ should thus be as large as possible in order to make use of the highest dc beam power density and consequently the strongest deflected reference upon reconstruction. Thus, $\hat{x} = x$ and y MAX = h MAX.

2.2 --Continued

It can be seen that

$$y\ MAX = w - xw/2f$$

and

$$h\ MAX = (b - c/e + f)(\hat{x} + e) + c$$

Thus,

$$w - \hat{x}w/2f = (b - c/e + f)(\hat{x} + e) + c$$

and

$$\hat{x} = \frac{w - c - e(b - c/e + f)}{(b - c/e + f + w/2f)}$$

The optimum placement is thus dependent on the characteristics of the Bragg cell (w,c,b), the Fourier transform lens (f,e,b,c), and d. All of these parameters, except c, are usually fixed and d is kept as small as possible to minimize the total path length. The distance $\hat{x}$ is largest in the case of the smallest c. Since c is directly related to the detected signals time delay through the system, the optimum placement occurs at the smallest time delay.

Using a zero time delay and applying the above equations to the actual lab set-up, the calculated maximum $\hat{x}$ is 752 mm for a zero time delay, the resulting K is 36%. The placement actually used was somewhat smaller, the time delay implemented ranging between 400 ns and 1.2 μs out of a maximum of 5 μs. The value of K or fraction of undiffracted light used to illuminate the hologram was approximately 28% with a delay of 1.2 μs.

2.3 HOLOGRAM DEVELOPING

The type of plates exposed were Kodak 120-02 .040- and .250-inch glass photographic plates and Kodak 649F .040 inch plates backed with an anti-halation

2.3 --Continued

coating. These plates exhibit low granularity or grain noise and high resolving power (greater than 2000 lines/mm). Steps taken to process these plates are listed below:

1) 7 minutes with gentle agitation in D-19 (400 $m\ell$ of Kodak D-19 concentrate per 2 ℓ of warm tap water.
2) 1 minute in 1.3% solution of acetic acid.
3) 4 minutes in Kodak rapid fix and hardener.
4) 30 seconds in "Hustler" brand rapid bath hypo-remover solution.
5) 5 to 10 minutes in running tap water.

NOTE: All solutions were made with normal tap water.

2.4 DIFFRACTION EFFICIENCY

In order to obtain a measure of each holograms performance, it was desirable to determine the diffraction efficiency which is the percentage of laser light diffracted by the hologram and forms the local oscillator beam. With the cylindrical lens removed from the optical path in Figure 2, the following measurements were performed:

Diffraction Efficiency $\triangleq P_1/P_{TOTAL}$

Relative Diffraction Efficiency $\triangleq P_1/P_o$

Hologram Average Transmission $\triangleq EP's/P_T$

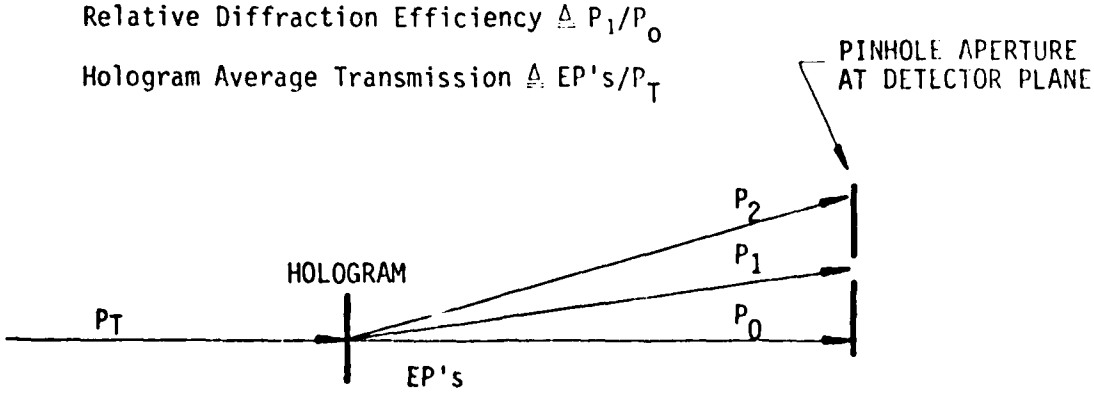

2.4 --Continued

where

P_1 = Power deflected in the first order
P_2 = Power deflected in the second order
P_0 = DC power, the light undeflected by the hologram
EP's = Total light through the hologram
P_T = Total light falling upon the hologram

Higher orders diffracted, mainly the second order, shown above, can impose problems. Any such order of appreciable magnitude forms a separate reference beam, causing multiple signals at the output of the detector. These higher orders are due to exposures in the non-linear portion of the films characteristic (resulting density vs. exposure energy) curve but can be kept to reasonably insignificant levels through proper exposure, resulting in operation on the linear portion of the curve.

2.5 HOLOGRAM EXPOSURE

The best exposure obtained for the Kodak 120 plates was approximately 30 $\mu J/cm^2$ as can be seen in the graph of Figure 4. This graph shows the diffraction efficiency obtained for different exposure levels at two different signal reference ratios - 2 to 1 and 10 to 1. Since the better efficiency is obtained with the smaller ratio, all the remaining 120 holographic plates were exposed with a low signal reference ratio.

The 649F plates proved to be more sensitive to exposure levels. A 30 $\mu J/cm^2$ was not sufficient to expose the plates and 90 $\mu J/cm^2$ produced an extremely dense exposure. Holograms with exposures of 60 $\mu J/cm^2$ achieved diffraction efficiencies comparable to the Kodak 120 holograms, however the 649F plates were less dependent on signal reference ratios. No appreciable difference, either in diffraction efficiency or overall performance was noticed in 649F holograms produced with 60 μJ exposure levels and signal reference ratios of 1 to 1, 5 to 1 and 10 to 1.

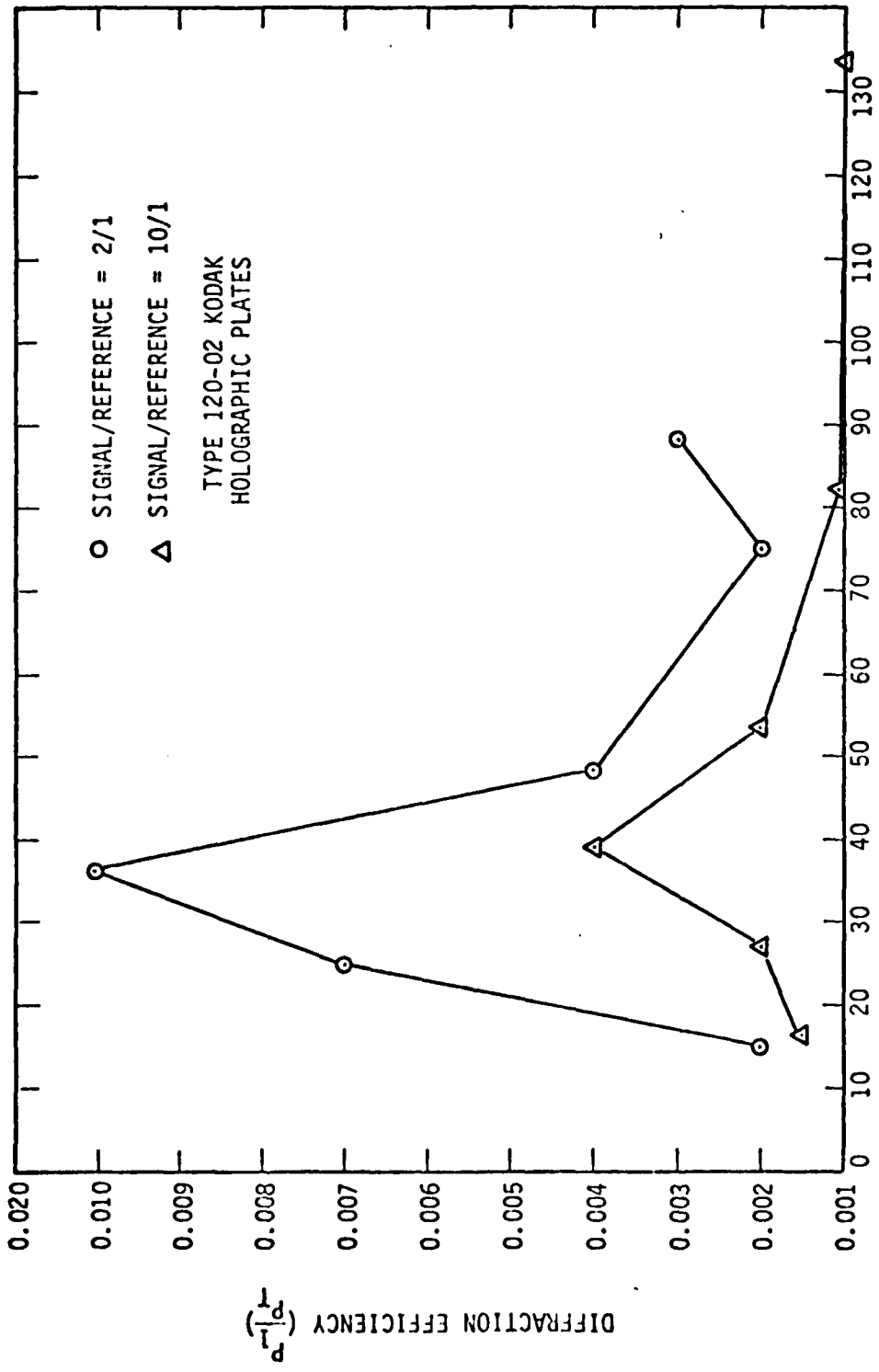

FIGURE 4 HOLOGRAM DIFFRACTION EFFICIENCY

PSI-80018

SECTION 3
PERFORMANCE MEASUREMENTS

3. PERFORMANCE MEASUREMENTS

This section of the report describes the performance measurements made to evaluate the holographic local oscillator technique. The most important performance measure of the optical processor for this evaluation was the maximum signal-to-noise ratio (SNR) that could be achieved without introducing detectable non-linear effects. To normalize out other factors in the optical processor components and alignments, the maximum SNR with hologram was compared directly with the maximum SNR with the conventional mirrors and beam-splitters. Other performance measures included multiple responses, frequency response and phase distortion.

3.1 COHERENT DETECTION WITH MIRRORS AND BEAM-SPLITTERS

To compare the hologram with conventional techniques, the optical system shown in Figure 5 was set up and measurements were taken to determine the best performance of the separate LO system as measured by the maximum output signal-to-noise ratio in a 30 KHz bandwidth. The variable beam-splitter and optical attenuator allow an adjustment of the ratio of signal-to-reference beams falling upon the cylindrical lens in both paths. With the total laser power kept constant, the detectors output SNR was evaluated at five different Bragg cell input levels of a 40 MHz CW tone for various system beam ratios. The Bragg cell used in this set-up was an Anderson Laboratories BD-125, 100-spot beam deflector with a 25 MHz bandwidth centered at 40 MHz. The input levels ranged from 3 dB below the level that caused the detector to saturate to 44 dB below the maximum input level. The results appear in the graph of Figure 6 and indicates that the best performance is obtained with a system signal-to-reference ratio of about unity achieving an output SNR of 48 dB for operation on signals 3 dB below the maximum input.

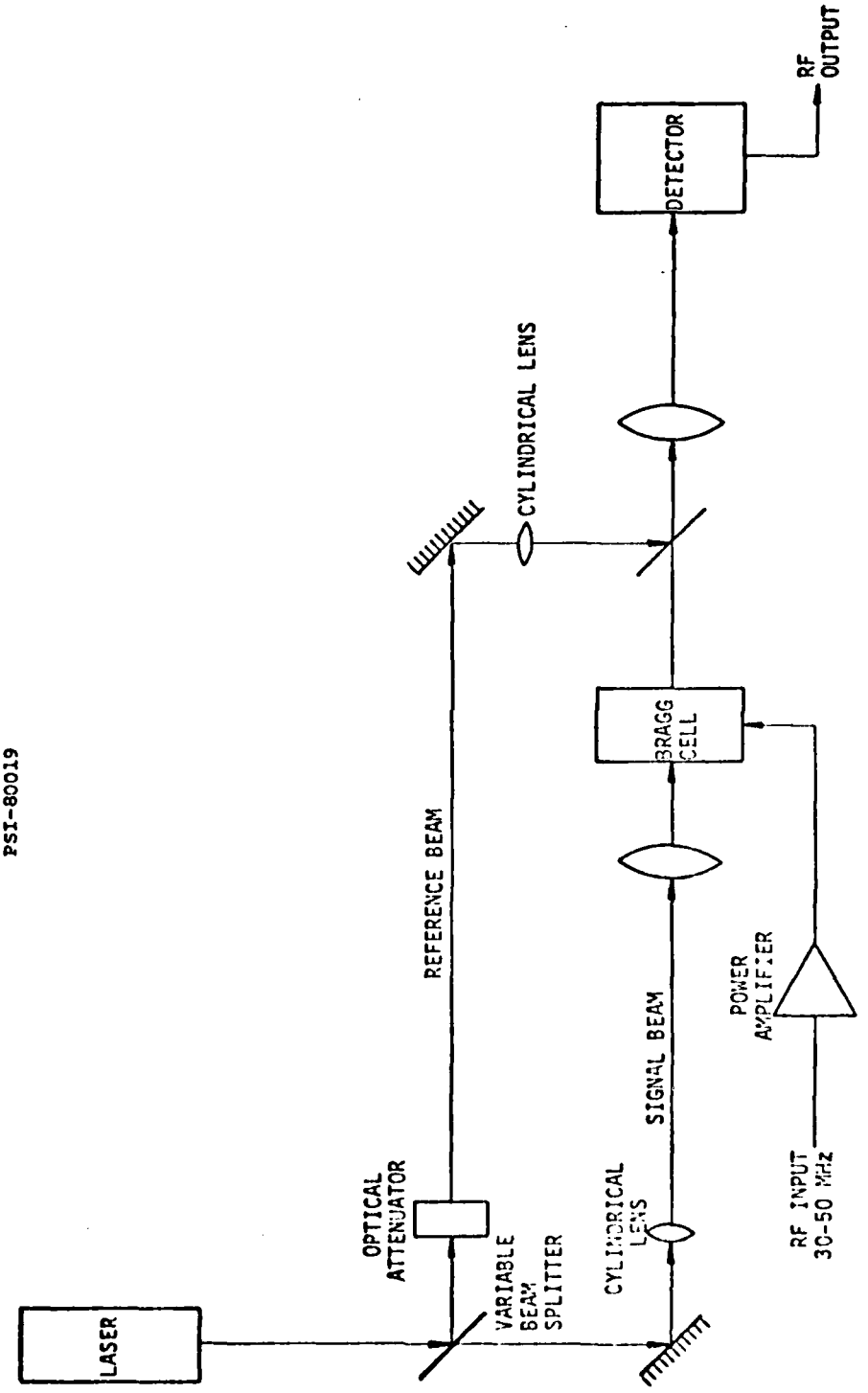

FIGURE 5 COHERENT DETECTION WITH SEPARATE LO

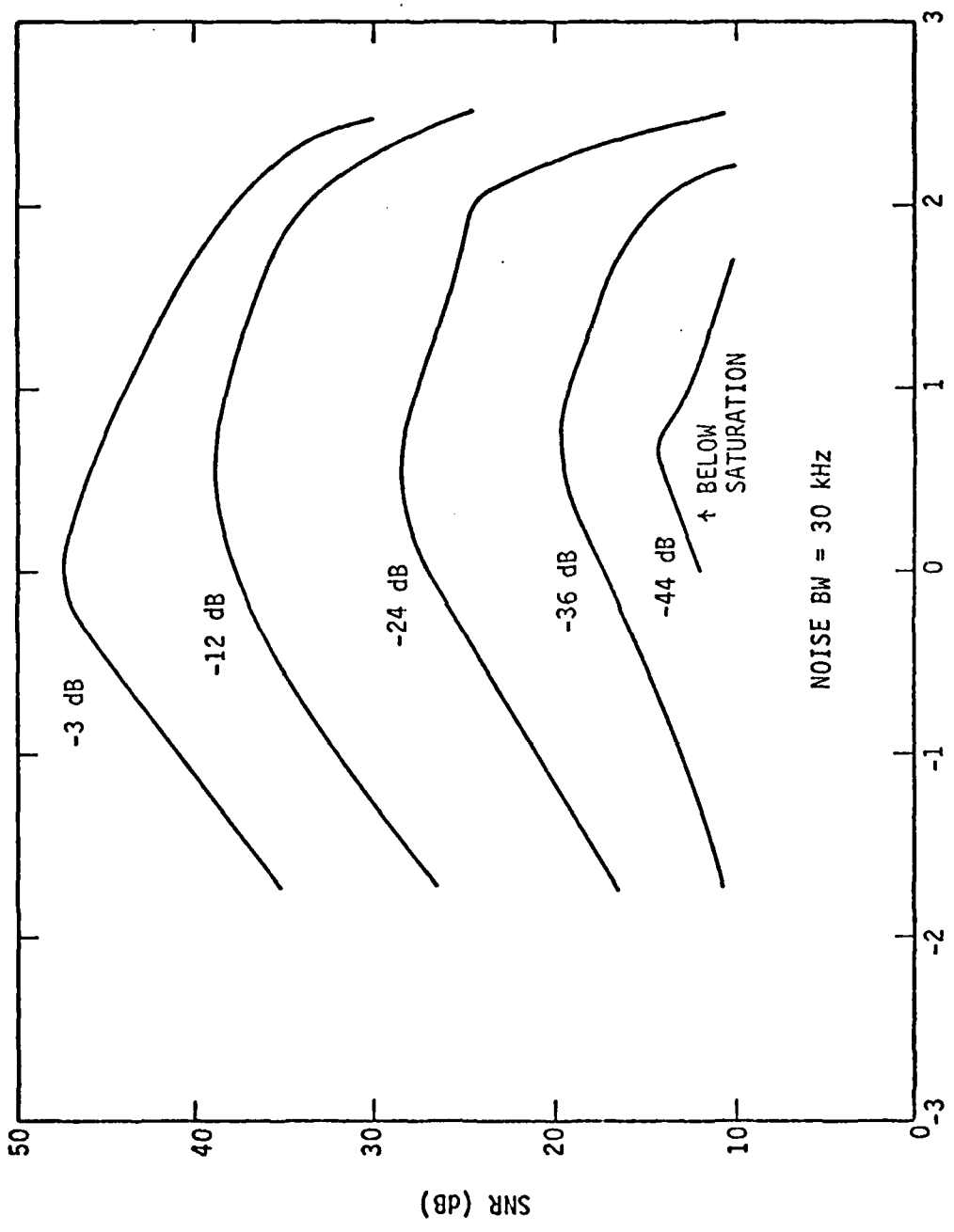

PSI-80020

FIGURE 6

OUTPUT FOR SEPARATE LO SNR VS. RATIO OF SIGNAL TO REFERENCE BEAM FOR VARIOUS INPUT LEVELS

3.1 --Continued

With a signal-to-reference ratio of 4, output signal and noise were measured for different input signal levels at the systems center frequency. These measurements appear in the graph of Figure 7 and show a slight noise compression beginning at approximately 0 dBm. At this input level, the output SNR is 42 dB. However, ignoring this apparent soft saturation of the detector, the maximum output SNR is 53 dB with a 10 dBm input signal.

3.2 COHERENT DETECTION WITH HOLOGRAMS

The diffraction efficiencies obtained with the properly exposed and developed Kodak 120 plates ranged between 1.5 and 2.7%, the relative diffraction efficiency between 13 and 24%, with the resulting average transmission at approximately 18%. The hologram with the best measured diffraction efficiency (2.7%) was placed in the optical set-up of Figure 2 and for various Bragg cell input levels of a 40 MHz, CW, the output signal and noise were evaluated at different system laser power levels. The results of these measurements appear in Figure 8 and show a maximum SNR of 47 dB for linear operation on high level signals with full laser power.

Decreasing the laser power causes a stonger input signal to bring the detector to the point of saturation (non-linear portion of the curve), however, at the expense of a decreased output signal. Decreasing the power by 2 dB (to 3 mw) increased the maximum input by 4 dB with a 3 dB drop in output signal and decreasing it by 7 dB (to 1 mw) increased the maximum input by 8 dB with a 6 dB drop in output power. The maximum SNR did not fall as sharply as the output signal due to the fact that the output noise level also decreased with lower laser power. The net effect is a 46 and 45 dB maximum SNR with laser levels 4 and 7 dB below the maximum of 4.5 mw. The holograms exposed on 649 plates exhibited about the same diffraction efficiency as the Kodak 120 plates (1.5-2.6%). However, the average transmission of these plates was approximately 33% -- almost double that obtained with the Kodak 120 plates. This higher average transmission results in a lower input signal necessary to saturate the detector

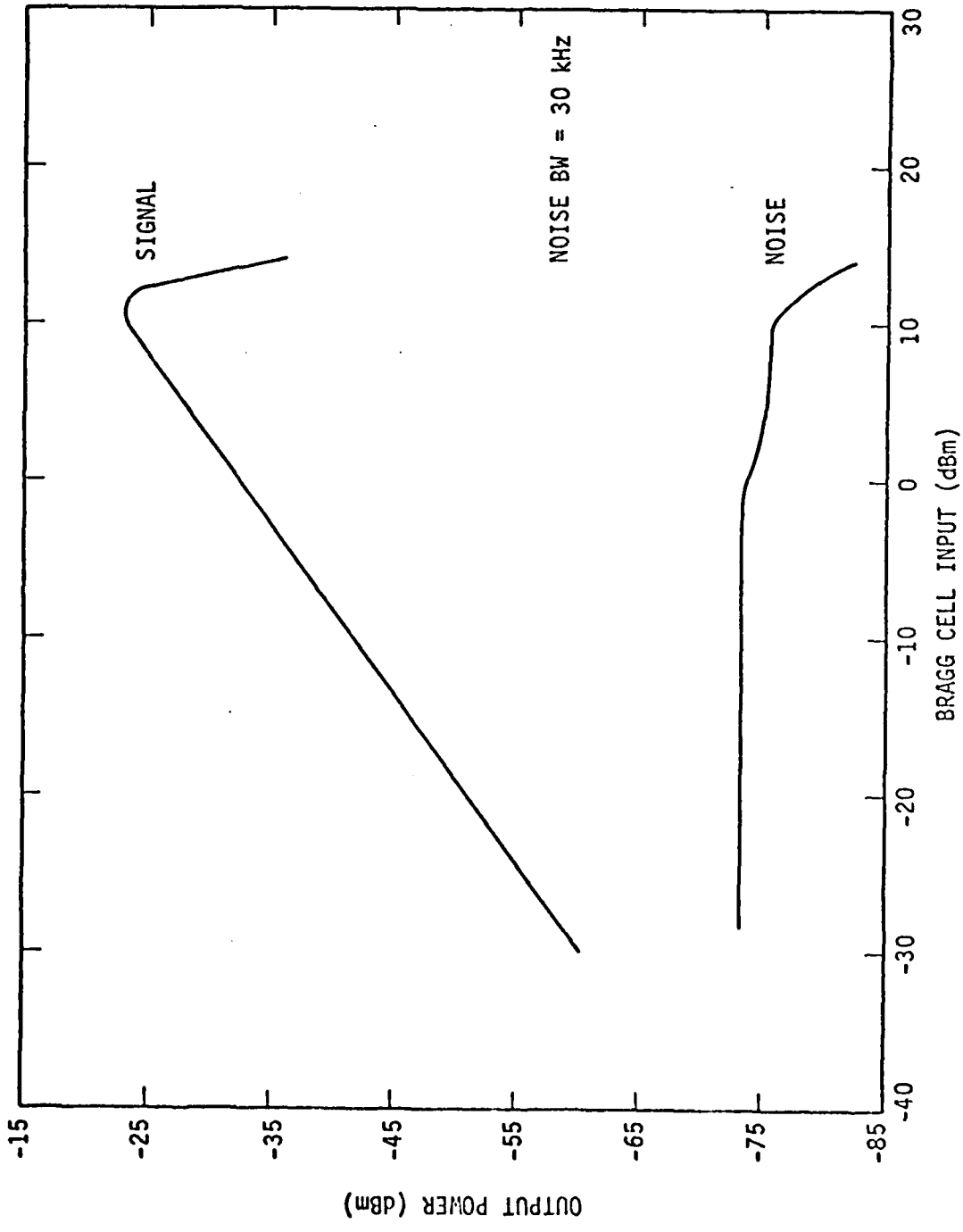

PSI-80021

FIGURE 7 SEPARATE LO OUTPUT SIGNAL AND NOISE POWER VS. INPUT AT CENTER FREQUENCY

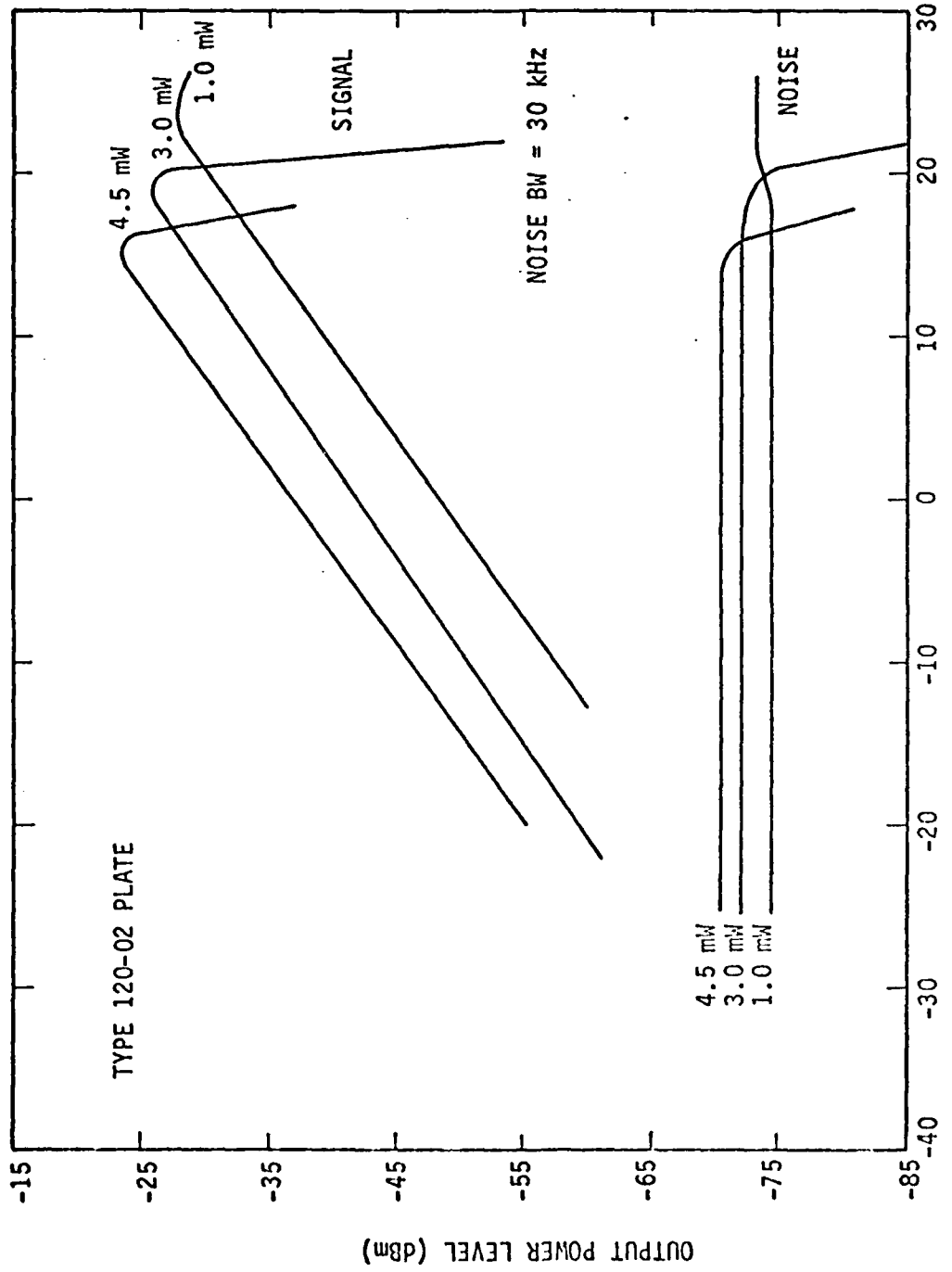

FIGURE 8
HOLOGRAPHIC LO OUTPUT SIGNAL AND NOISE POWER VS. INPUT
AT CENTER FREQUENCY FOR THREE LASER OUTPUT LEVELS

PSI-80022

3.2 --Continued

and should move the curve in Figure 8 to the left, causing a 3 dB rise in processing gain. This can be seen in the curve of Figure 9 which shows the output characteristics of a 649F hologram with a diffraction efficiency of 2.6%. With the output SNR remaining approximately constant due to equal diffraction efficiencies, it is desirable to obtain the highest average transmission possible. The higher the average transmission of the hologram, the higher the percentage of optical signal that reaches the detector and thus, a smaller Bragg cell input causes the detector to saturate. The limiting factor in the systems dynamic range is the saturation of the detector. Should a detector capable of handling higher optical signal levels become available, the maximum system input could increase to 34 dBm, the maximum input rating for the Anderson Lab Bragg cell used in these measurements.

It should be noted that all the holograms within the diffraction efficiency range indicated above exhibited similar characteristics with the output signal power varying at most 3 dB between holograms and the input level which brought on saturation differing no more than 1 dB.

Comparing the graphs of Figure 8 and 9 with those of Figures 6 and 7 it is clear that the holographic technique as implemented in the manner previously described can achieve an output SNR comparable to that of the separate LO approach. The use of the 649F plate, whose system characteristics are shown in Figure 9, provided a 47 dB output SNR with an input 3 dB below saturation - the same SNR resulting from equal reference and signal beams in the separate LO technique.

3.3 MULTIPLE SIGNALS

Although second and third order diffractions were observed falling upon the detector, no multiple signals were observed at the output. To illustrate that the holographic technique did not seriously degrade the coherent detection

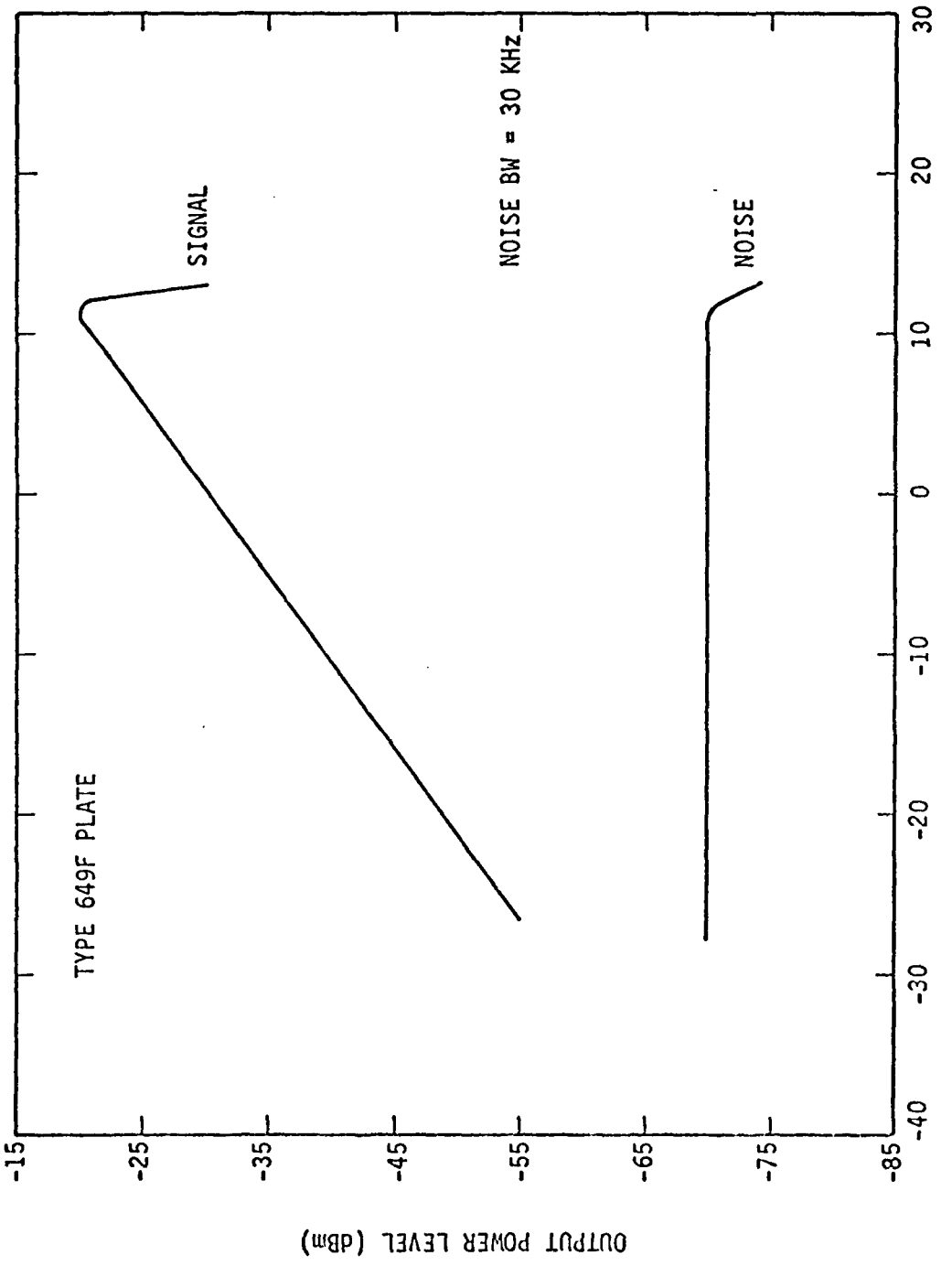

PSI-80023

FIGURE 9 HOLOGRAPHIC LO OUTPUT SIGNAL AND NOISE POWER VS. INPUT AT CENTER FREQUENCY

3.3 --Continued

process, the following photographs were taken with the use of the hologram whose signal and noise characteristics are depicted in Figure 9. All the holograms exhibited the same performance, with the exception of an amplitude variation on the output due to slightly different diffraction efficiencies and average transmissions between holograms.

Figure 10 shows the input and output of a 1 μs 40 MHz pulse with a pulse repetition interval of 4.2 μs. Figure 11 shows the same with the output display raised by 20 dB. Figures 12, 13, 14, and Figure 15 show pulses of various widths, all of which can be seen to be of high signal-to-noise ratios and show no ill effects due to the holographic LO. Vibrations manually applied to the optical components which would cause tremendous jitter on the output pulses of the separate LO system are barely noticeable on the output of the holographic system.

To emphasize the importance of the placement of the hologram, Figure 16 shows the output with the hologram shifted in the vertical direction. This shift causes the higher orders to be detected and consequently multiple and distorted pulses occur at the detector output.

3.4 FREQUENCY RESPONSE

To examine the effects the holographic technique had on the system's frequency response, a 10 dBm signal was applied to the Bragg cell and the output signal power measured for frequencies between 26 and 54 MHz. The resulting output spectrum of Figure 17 is relatively flat, exhibiting a little over a ± 1 dB ripple from 30 to 50 MHz. Note that by taking the average response across the spectrum, the 3 dB bandwidth is 21 MHz. Although the Bragg cell has a 25 MHz bandwidth, the systems bandwidth was reduced to 21 MHz by reducing the detector aperture. This response does not differ significantly from that obtained with the separate LO detection scheme.

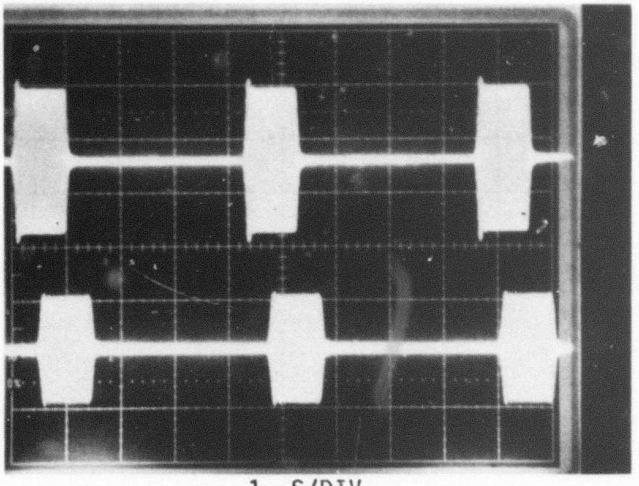

FIGURE 10 1-μS PULSE AT 40 MHz

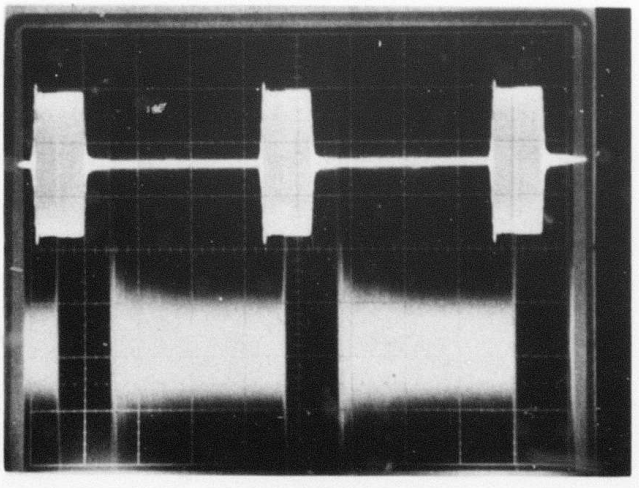

FIGURE 11
1-μS PULSE AT 40 MHz WITH OUTPUT RAISED BY 26 dB

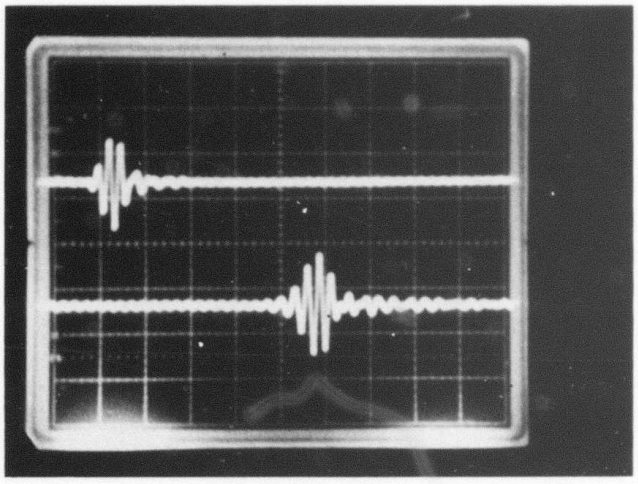

FIGURE 12 70-NS PULSE AT 40 MHz

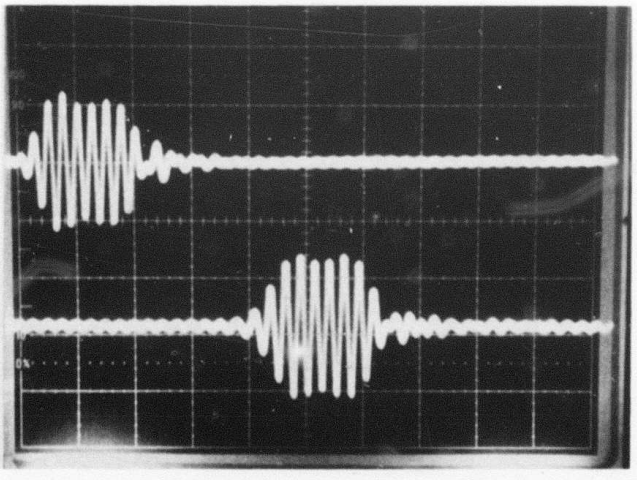

FIGURE 13 210-NS PULSE AT 40 MHz

0.5 V/DIV

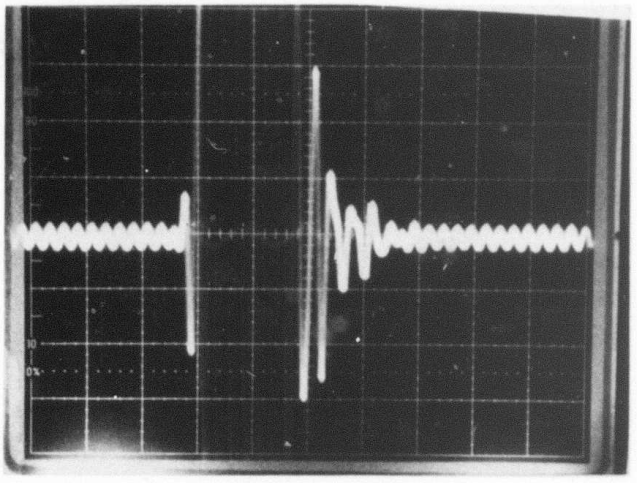

100 NS/DIV

FIGURE 14

INPUT PULSE AT 40 MHz RAISED BY 20 dB
ABOVE THE DISPLAY IN FIGURE 13

20 MV/DIV

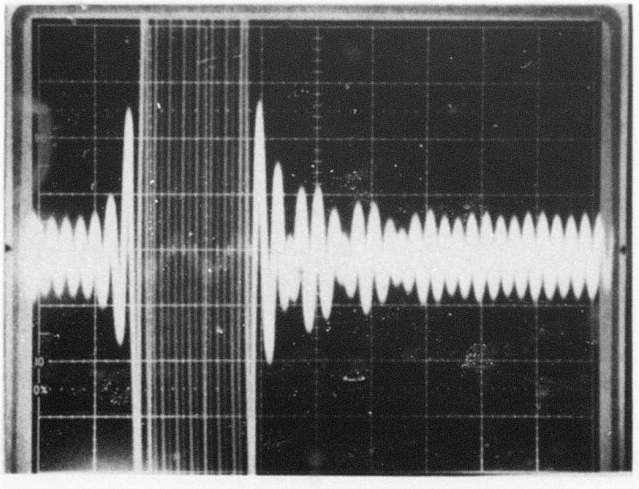

100 NS/DIV

FIGURE 15

OUTPUT PULSE AT 40 MHz RAISED BY 20 dB
ABOVE THE DISPLAY IN FIGURE 13

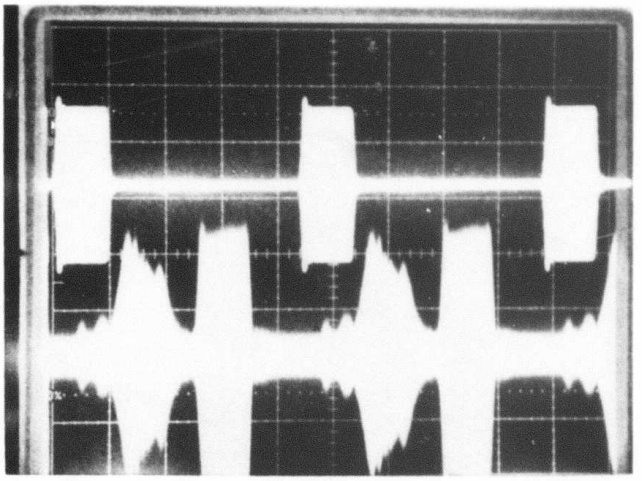

FIGURE 16

MULTIPLE PULSES BECAUSE OF IMPROPER
PLACEMENT OF HOLOGRAM

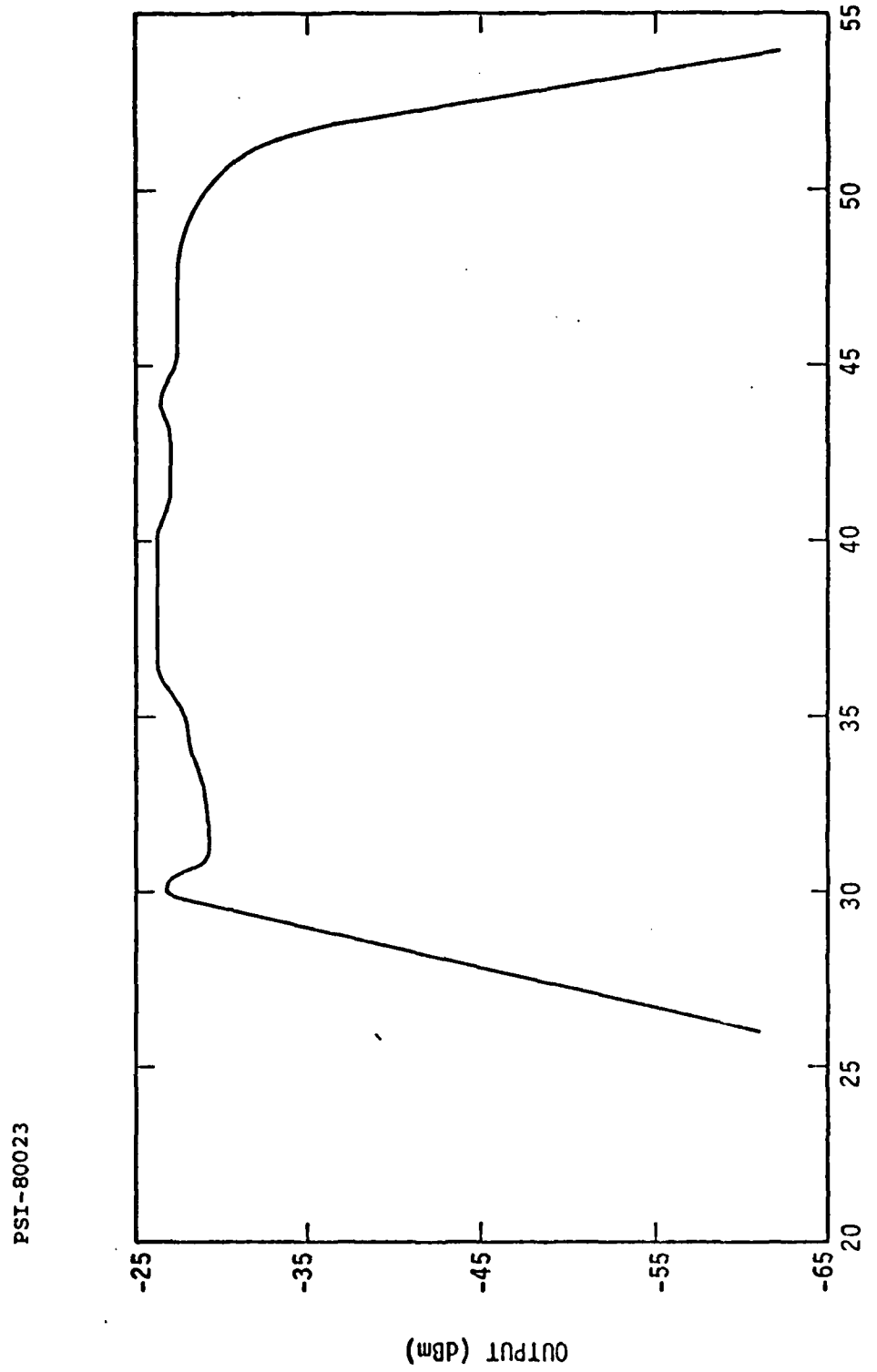

FIGURE 17 FREQUENCY RESPONSE OF HOLOGRAPHIC TECHNIQUE

3.4 --Continued

With a CW 40-MHz input signal, the detector output was placed on a RF spectrum analyzer set at a 30 KHz bandwidth and is shown in Figure 18.

3.5 PHASE ERRORS

Using the delayed trigger on a Tektronix 465 oscilloscope with a single tone input, the phase errors were examined as a function of frequency by observing the time delay differences as a function of frequency. Within a measurement error of $\pm 30^{\circ}$, the phase was flat from 30 to 50 MHz for the Kodak 120-02 thick plates and within 50° for the 649F and 120 thin plates.

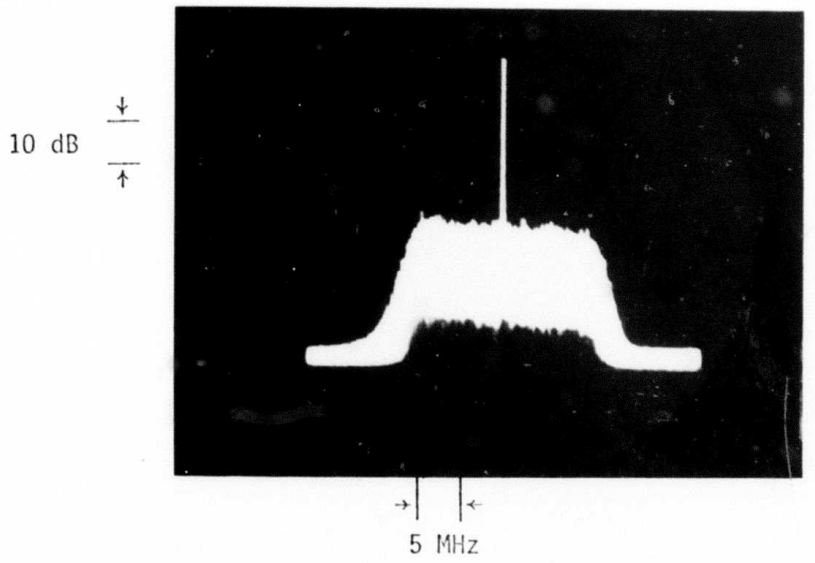

FIGURE 18
OUTPUT SPECTRUM FOR A 40-MHz INPUT SIGNAL

SECTION 4
CONCLUSIONS AND RECOMMENDATIONS

4. CONCLUSIONS AND RECOMMENDATIONS

The results presented in this report demonstrate the feasibility of using a hologram to replace the mirrors and beam-splitters needed to coherently detect the optically generated spectrum of a broadband signal. The performance of the optical processor used in the experiments was equal to or better with a hologram than with the mirrors and beam-splitters. The most significant improvements were in the ease of alignment and the freedom from excess noise due to microphonics and laser coherence.

Recommendations for future work are included in two areas of research and development. First, considerable development will be required to mature the holographic technique into an industry standard. Engineering design measurements are needed to determine the optimum diffraction efficiency as a function of the optical processor specifications. Existing literature provides some of the insight needed to answer questions such as chromatic aberrations, wave-length scaling, and double diffraction effects but more work is needed to apply this background to coherent optical processors. Investments in this development effort would provide engineers the procedures and design data needed to properly process, install and test holograms for future optical processors.

The second area of investment should be in the research of holograms capable of generating non-spherical wave-fronts for the local oscillator beam. Various signal processing functions should be possible with non-standard holograms. For example, the output signal in Figure 16 shows that the time wave-form of a signal can be changed in a predictable manner. This effect could be used for pulse compression, correlation, and frequency filtering. A well-planned research program would concentrate on the identification of signal processing techniques previously thought to be impossible because of the enormous amount of computing required to implement the functions with digital hardware. A coherent optical processor could be a simple solution to signal processing problems that have not yielded to conventional approaches.